esa

ECOSPHERE

Temporal dynamic analysis of a mountain ecosystem based on multi-source and multi-scale remote sensing data

Edurne Ibarrola-Ulzurrun,[1,†] Javier Marcello,[1] Consuelo Gonzalo-Martín,[2] and José Luis Martín-Esquivel[3]

[1]*Instituto de Oceanografía y Cambio Global (IOCAG), Universidad de Las Palmas de Gran Canaria (ULPGC), Parque Científico Tecnológico Marino de Taliarte, 35214 Telde, Las Palmas, Spain*
[2]*Department of Computer Architecture and Technology, Universidad Politécnica de Madrid (UPM), Campus de Montegancedo, Boadilla del Monte, 28660 Madrid, Spain*
[3]*Parque Nacional del Teide, C/Sixto Perera González 25, 38300 La Orotava, Tenerife, Islas Canarias, Spain*

Citation: Ibarrola-Ulzurrun, E., J. Marcello, C. Gonzalo-Martín, and J. L. Martín-Esquivel. 2019. Temporal dynamic analysis of a mountain ecosystem based on multi-source and multi-scale remote sensing data. Ecosphere 10(6):e02708. 10.1002/ecs2.2708

Abstract. During the last decades, ecosystems have suffered a decline in natural resources due to climate change and anthropogenic pressure. Specifically, the European rabbit introduced by humans, as well as drought episodes, have led to a change in the vegetation structure of a mountainous ecosystem: Teide National Park in Spain. Teide managers studied, with field-based traditional methods, how the two keystone vegetation species, *Spartocytisus supranubius* and *Pterocephalus lasiospermus,* have changed their dynamics in this vulnerable and heterogenic ecosystem. However, remote sensing is an important tool for classifying, monitoring, and managing large areas in a fast and economic way. This work proposes a methodological framework to monitor the changes produced in this protected area using multi-source remote sensing imagery. The results strengthen and extend the analysis followed by the National Park managers, demonstrating that *S. supranubius* has decreased its population while *P. lasiospermus* has increased. Moreover, this study presents thematic maps of the species of interest, as well as its specific coverage at different dates, providing quantitative data difficult to get with traditional approaches.

Key words: change detection; hyperspectral imagery; invasive species; multispectral imagery; remote sensing imagery; support vector machine.

Received 11 March 2019; accepted 18 March 2019. Corresponding Editor: Debra P. C. Peters.

† **E-mail:** edurne.ibarrola101@alu.ulpgc.es

Introduction

Ecosystems are exposed to high pressure due to intensification of agricultural land use, tourism, development, and climate change, being highly dynamic in space and time. Specifically, climate change is producing important variations in entire communities in those areas where it manifests most intensely, such as regions at greater latitude and areas of higher altitude. Thus, ecosystem deterioration has a strong negative impact in the local biodiversity and might put rare and threatened species at a serious extinction risk (Pepin and Lundquist 2008, Spanhove et al. 2012).

In this context, to understand ecosystem dynamics and its consequences is vital for the success of their conservation and restoration, especially on the services they provide (Mueller and Geist 2016). Thus, it is important to implement accurate monitoring methodologies of land surface attributes, as it is critical for dealing with uncertainty in the management of large ecosystems (Coppin et al. 2004, Förster et al. 2014). Hence, for large-scale monitoring efforts, two general approaches have been defined (Manley et al. 2000): retrospective and predictive. Retrospective monitoring seeks to detect changes in status or condition, while predictive monitoring seeks to detect indications of undesirable effects before they have a chance to occur or become serious. Both retrospective monitoring and predictive monitoring deal about detecting changes in a large-scale area. In that regard, change detection could be defined as the process of identifying differences in the state of a phenomenon at different times (Singh 1989). The time and accuracy of change detection on the Earth's surface can provide guidance for resources management by using multi-temporal datasets related to state of changes (Lu et al. 2004).

An ecological monitoring program should ideally consider ecological relevance, statistical credibility, cost-effectiveness, flexibility, and transferability to other systems, as the most important criteria (Mueller and Geist 2016, Mason et al. 2017). In this context, remote sensing could be an important tool to monitor ecosystems, at community and species level to detect population trends, that guide in the establishment of conservation objectives with the purpose of avoiding the transition to undesirable situations (Mason et al. 2017).

Remote sensing can contribute to a better understanding of natural habitats, their spatial distribution, and their conservation status, being considered an ideal data source for land-cover classifications in large areas (Corbane et al. 2013). Hence, it is a valuable tool for monitoring and managing ecosystems, as it allows the acquisition of data in remote and inaccessible areas (Spanhove et al. 2012, Förster et al. 2014). Besides, it has been successfully used for many ecological studies, such as detecting land-cover changes, monitoring crops, deforestation, forest fires, estimating carbon sequestration, detecting vegetation stress, and other applications (Aplin 2004, Spanhove et al. 2012, Alqurashi and Kumar 2013). This technology is important since traditional field-based assessment methods are sometimes subjective, time-consuming, data lagged, and often too expensive. Thus, remote can complement and add information to traditional field-based methods providing indicators for different spatial and temporal scales and involving varying temporal revisit frequencies up to daily observations (Xie et al. 2008, Nunez-Casillas et al. 2012, Förster et al. 2014).

The area of study is the Teide National Park (Tenerife, Spain), a vulnerable high mountain ecosystem strongly stressed by climate change. This study describes a methodology framework to monitor non-herbaceous species of these ecosystems using remote sensing imagery. The conservation managers have analyzed how the two keystone species have changed their population dynamic due to the abundance of European rabbits and recurrent drought episodes. Specifically, the study proposes a post-classification analysis to study those dynamics by using remote sensing multi-source and multi-temporal data, in order to complement and add accurate information to the field observations, for a future ecosystem management.

Study Case Description

Study area

The study area is a high mountain ecosystem in the subtropical island of Tenerife (28°06′ N 15°24′ W), the Teide National Park with 13,679 ha of total extension. The dominant vegetation is a meso-oromediterranean shrub dominated by the endemic broom, *Spartocytisus supranubius* (del Arco Aguilar et al. 2010) (Fig. 1).

The National Park is formed by a large caldera, inside which the Teide volcano rises up to an altitude of 3718 m, being the highest peak of Spain. According to the records in the database of the Teide National Park, a total of 206 vascular plants, mostly herbaceous, acclimated to the stressed environmental conditions of high altitude, grow there. Of these taxons, 7% are endemic from Teide National Park, whereas the 15% are endemic from Tenerife and 32% are endemic from Canary Islands. The adaptations to the altitude of these species are manifested in the shape of the leaves (Lausi and Nimis 1986), and the canopy and the physiology of the plants (Perera-Castro et al. 2017*b*), which have been well studied in the case of the *Spartocytisus supranubius* (Teide broom) (González-Rodríguez et al. 2017) and the pine *Pinus canariensis* (Canary pine) (Brito et al. 2014). Indeed, *S. supranubius* is one of the most important plant species, as well as

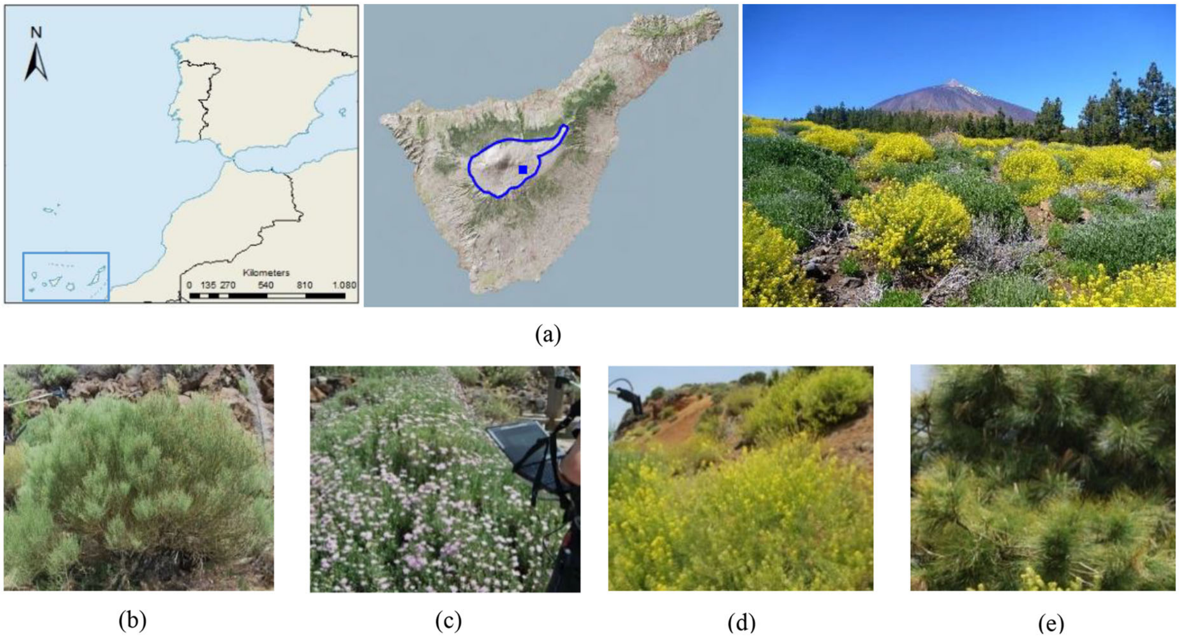

Fig. 1. (a) Teide National Park, location and species of interest: Blue line delimits the total National Park and the blue square the study area. (b) *Spartocytisus supranubius*, (c) *Pterocephalus lasiospermus*, (d) *Descurainia bourgaeana*, and (e) *Pinus canariensis*.

P. canariensis, *Descurainia bourgaeana* (Hierba pajonera), and *Pterocephalus lasiospermus* (Rosalillo de cumbre). The latter is particularly surprising, since in the middle of the last century, it was considered a very rare species, of which only a few specimens were known (Sventenius 1946). However, nowadays, it is the most abundant species in the National Park, possibly due to its thermophilic character (Perera-Castro et al. 2017*a*) and its low palatability for herbivores (Cubas et al. 2018). Fig. 1 shows the species selected to the study.

Ecosystem description and problematic

The Teide National Park has been historically the object of several human uses, mainly led by the grazing of goats and the extractive activities of soil and wood of *S. supranubius*. Nowadays, goats have been eradicated, while extraction of wood is considered a traditional activity of low intensity, being beekeeping the only remaining activity. The greatest current challenges for the management of the Park are public use, herbivory pressure due to rabbits and droughts episodes, and temperature increase (climate change). Regarding public use, it is about making compatible the enjoyment of nature, by more than four million visitors a year, with its conservation.

The presence of herbivores continues to be a factor of pressure on the flora, especially the European rabbit (*Oryctolagus cuniculus*). The rabbits were introduced on Canary Islands during 15th–16th centuries by the Castilian conquerors, but their populations have increased in the last decades, reaching densities of up to 3 rabbits/ha some years, because the climate in the summit is becoming less cold (Martín et al. 2012). They play a key role in the functioning of the ecological systems (Chapuis et al. 2004). *Oryctolagus* affects ecosystems by producing changes in the structure and composition of the soil, as well as in the richness and diversity of plant species. Cubas et al. (2018) studied how rabbits influenced the population dynamics of two of the most abundant plants of this habitat, *S. supranubius* and *Pterocephalus lasiospermus*, demonstrating an antagonistic effect: While rabbits limited the expansion of *S. supranubius* because when feeding on their seedlings prevented the regeneration of the plant, at the same time they favored the expansion of *P. lasiospermus* because this plant was able to take advantage of the extra nutrients contribution from the latrines of the herbivore and it was less palatable than the brooms. This study was made in small areas of the Park through traditional field-based assessment methods.

Spartocytisus supranubius is the key species of the high mountain ecosystem of Tenerife. Its populations were reduced at the beginning of the last century until the declaration of the Teide National Park led to the suppression of pastoral activities in the sixties. Since then, their populations experienced a considerable recovery; however, this positive trend slowed down in the 1980s, when episodes of death began to appear matching with a strong increase in temperature, drought episodes, and, probably, an increase in rabbit populations. Extinction events of *S. supranubius* affect the entire National Park but are most notable in the southern area where extreme drought severely reduced the secondary growth of brooms (Olano et al. 2017, Cubas et al. 2018). The dendrochronological analyses, elaborated by Olano et al. (2017), studied the impact of the droughts of 2008 and 2012, underlining that they were important stress factors behind the death of *S. supranubius*.

Remote sensing can complement and add relevant information to Cubas et al. (2018) work, covering a larger area of study and quantifying the surface area of the same species considered in this study, as well as other important species of the Teide National Park.

Remote sensing framework

Remote sensing involves measuring electromagnetic radiation from features on the Earth's surface, providing a basic representation of land-cover variation (Aplin 2004). In this context, change detection is one of the most important applications in remote sensing (Mouat et al. 1993, Petit and Lambin 2001, Volpi et al. 2013). It aims to identify the changes occurred by jointly analyzing two or more images over the same geographical scene at different times (Gong et al. 2016).

The ideal situation would be to have data from the same sensor, same dates during different years and under same conditions; however, this is not always possible, so the use of multi-source data is the best approximation. In fact, the integration of multi-source and multi-temporal remote sensed imagery is one of the most challenging tasks and an active area in the field of change detection (Lu et al. 2004, Jianya et al. 2008, Volpi et al. 2013, Gong et al. 2016). Moreover, the use of multi-source images for change detection is worth to be considered and researched deeply, while multi-temporal imagery has the potential to compensate for possible bias in the spectral information caused by the plants being in different phenological phases.

Besides, the type of imagery is a major factor in the classification analysis, and hence, in change detection studies. The evolution of space-borne remote sensing has led to the introduction of advanced multispectral (MS) and hyperspectral (HS) imagery from the visible to the near-infrared spectrum (400–2500 nm). Multispectral satellite imagery with three to eight bands is commonly used in land-cover classification, vegetation studies, texture, land-cover changes, forest fires, and others (Rodriguez-Galiano et al. 2012, Feilhauer et al. 2013). The launch, in the last decades, of high spatial resolution satellite sensors (i.e., IKONOS, QuickBird, WorldView) has been an advance of remote sensing in biodiversity analysis and monitoring. Also, for more heterogeneous ecosystems, such as the shrublands or tropical forests, high spatial resolution HS images are ideal for habitat monitoring (Jiménez-Michavila 2011) because the availability of tens to hundreds of spectral bands provides more information to discriminate and analyze the status of different species. The lack of HS satellite imagery with high spatial resolution has led to the use of airborne HS sensors. HS airborne imagery allows the simultaneous acquisition of spectral bands with high spatial resolution, increasing the possibility of accurately discriminating the land covers of interest (Fauvel et al. 2013, Ballanti et al. 2016). However, HS imagery is more expensive and requires higher computational cost.

In this context, classifying the species of the Teide National Park requires a spatial resolution less than 1 m in order to discriminate at species level due to the complexity of the ecosystem, with mixed vegetation and small shrubs. Therefore, the change detection study, covering 15 yr, was carried out using multi-source and multi-temporal data. Three different very high-resolution images were used in the study, two MS provided by the QuickBird (QB) and WorldView-2 (WV-2) sensors, and one HS recorded by the CASI 1550i sensor (compact airborne spectrographic imager) (Table 1, Fig. 2).

The date is an important factor in the selection of the imagery to be analyzed. Thus, the Teide images acquisition was done during the end of the spring season as the vegetation species have greater spectral separability.

Methodology

When implementing a change detection project, the following major steps are involved (Lu et al. 2004): (1) image pre-processing; (2) classification; (3) selection of suitable techniques to implement change detection analyses; and (4) accuracy assessment. The methodology framework followed in the study is shown in Fig. 3. It was implemented using ENVI 5.1 image processing software (Exelis Visual Information Solutions, Boulder, Colorado, USA) and MATLAB software (MathWorks, Natick, Massachusetts, USA).

Pre-processing

Prior to a land-cover change analysis, some pre-processing steps are necessary to standardize the multi-source and multi-temporal images. Remote sensors provide raw data images; thus, it is necessary to apply correction techniques and to perform image pre-processing in order to obtain high-quality imagery (Ibarrola-Ulzurrun et al. 2018).

Radiometric and atmospheric correction.—Apart from the radiometric calibration to convert digital numbers to radiance values, there are different ways of correcting remote sensing data for atmospheric effects: simple image-based methods and more complex algorithms based on a radiative transfer model of the atmosphere. In this work, complex models were applied: specifically, the fast line-of-sight atmospheric analysis of spectral hypercubes (FLAASH) to the satellite data (Marcello et al. 2016) and the atmospheric correction (ATCOR-4) to the airborne imagery (de Miguel et al. 2014).

Pansharpening and resizing.—High-resolution MS platforms record data simultaneously by using MS and panchromatic (PAN) sensors, providing both types of imagery of the same scene with different spatial and spectral resolution. The MS image is characterized by having higher spectral resolution, while the PAN image obtained from this sensor has a higher spatial resolution. Image fusion, or pansharpening, allows to improve the spatial quality of the MS image. Thus, the pansharpening data fusion technique is defined by the process of merging MS and PAN images to create new MS fused images with higher spatial resolution. This process is very important in the analysis of heterogeneous and mixed shrublands ecosystems, where the size of the plants to be analyzed is small.

After a detailed review of the state-of-art in pansharpening techniques, pansharpening algorithms achieving optimal performance were assessed and selected in previous studies performed for the Teide National Park (Ibarrola-Ulzurrun et al. 2017*a*, *b*). Thus, it was decided to use the Wavelet "à trous" algorithm to perform the pansharpening process in QB and WV-2 imagery to increase the spatial resolution by a factor of four with the minimum degradation of the spectral information.

The CASI imagery does not have a PAN image; however, as it appears in Table 1, its

Table 1. Specifications of the multispectral (MS) and panchromatic (PAN) images, QuickBird (QB) and WorldView-2 (WV-2), and the hyperspectral (HS) image, compact airborne spectrographic imager (CASI).

Image type	Spatial resolution	Spectral resolution	Acquisition date	Product	Reference
QB	MS: 2.4 m PAN: 0.65 m	4 MS bands 1 PAN band	26 May 2002	Orthoready	Digital Globe†
WV-2	MS: 1.85 m PAN: 0.48 m	8 MS bands 1 PAN band	16 May 2011	Orthoready	Digital Globe
CASI	0.75 m	68 HS bands	1 June 2017	Level 2c‡	de Miguel et al. (2014)

† https://www.digitalglobe.com/resources/satellite-information
‡ Level 2c: Radiometrically and atmospherically corrected, and orthorectified.

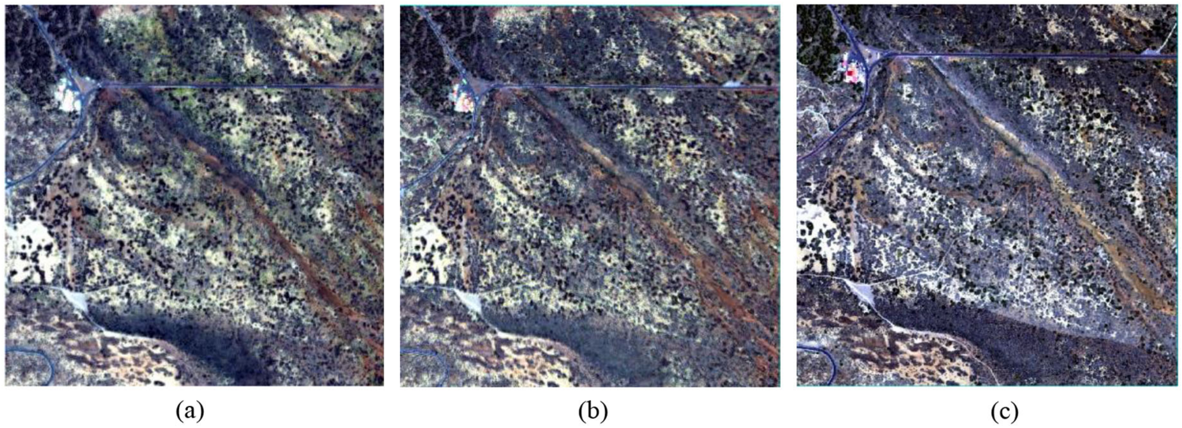

Fig. 2. Remote sensing imagery in RGB color composite: (a) QuickBird of 2002 (R: 3, G: 2, B: 1); (b) WorldView-2 of 2011 (R:5, G: 3, B: 2); (c) compact airborne spectrographic imager (CASI) of 2017 (R:29, G: 20, B: 12).

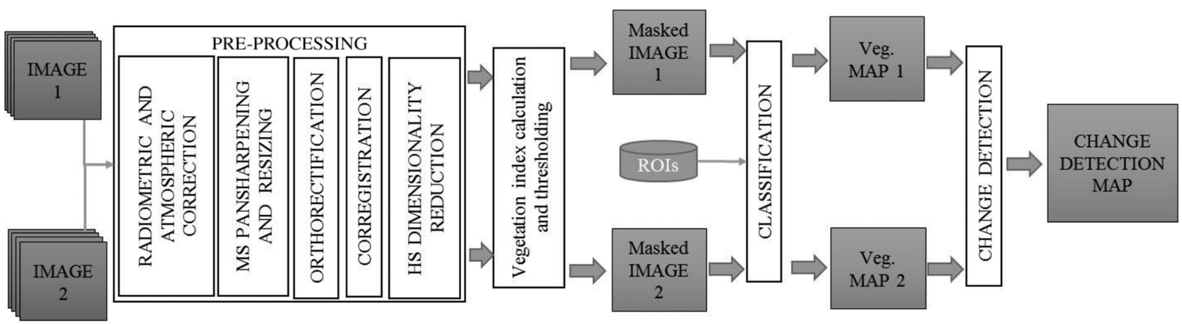

Fig. 3. Diagram followed in the change detection study.

spatial resolution is higher than both MS images (QB and WV-2) because CASI flies on board an aircraft instead of a satellite at much higher altitude. Thus, a pixel resizing was performed in order to obtain the same pixel size (0.5 m), using nearest neighbor algorithm (ENVI 2004), to avoid the mixing of information from neighboring pixels.

Orthorectification.—Orthorectification schemes were applied in order to minimize the distortions mainly induced by the topography. Some geometric error sources could be the variation of the movement in the platform and in the measuring instruments, the viewing angles of the sensor, the atmosphere conditions, Earth's curvature and rotation, topographic effects, etc. In this context, orthorectification was necessary as we are dealing with a mountainous ecosystem. A rational polymodal orthorectification (RPC) model was performed, which replaces the rigorous sensor model with an approximation of the ground-to-image relationship (ENVI 2004). The orthorectification errors in each scene were compared visually with images obtained from GRAFCAN (Cartografía de Canarias S.A.) and quantitatively with existing geodesic points (http://visor.grafcan.es/visorweb/). The CASI image was orthorectified by georeferenced hemispherical-directional reflectance factor (de Miguel et al. 2014).

Co-registration.—Image co-registration is the process of geometrically aligning two or more images. Precise co-registration of the images is required in change detection studies. The importance of accurate spatial co-registration is obvious because large spurious results of change detection will be produced if there is misregistration. It is difficult to achieve high accuracy in the co-registration between multi-temporal and multi-source images due to many factors, that is, imaging models, imaging angles, topography, curvature and rotation of the Earth or sensor type, and data acquisition. For these reasons, in a mountainous area, an orthorectification is needed first (Jianya et al. 2008), as it was performed in this study. The geometric relationship between the warp image to register and the base image was obtained through a number of representative and well-distributed tie points and, then, applying the corresponding geometric transform. In the case of this study, a minimum of 40 distributed ground control points (GCPs) were collected for each pair of images, considering the WV-2 data as the base image. A polynomial method was used with a nearest neighbor resampling (ENVI 2004) to fit the images in the overlapping areas.

Dimensionality reduction for CASI imagery.— Regarding HS image, due to the high number of spectral bands, an additional pre-processing step is sometimes required. HS classification is a challenging task due to the presence of redundant features, the imbalance among the limited number of available training samples for the supervised classification, and the high dimensionality of the data (Ghamisi et al. 2017). Therefore, the high level of data dimensionality in HS imagery poses a problem for classifications because of the unbalance between the high dimensionality of the input data and the number of training samples used in the supervised classification process, known as the "Hughes phenomenon" (Hughes 1968). Hence, when the number of spectral bands (dimensionality) increases, with a constant number of training samples, the accuracy of the statistics estimation decreases (Ghamisi et al. 2015). To solve this issue, data reduction through band selection decreases dimensionality without the need to increase the amount of training samples.

In a previous study, Ibarrola-Ulzurrun et al. 2017*c* compare the performance of different dimensionality reduction techniques and assessed strategies for selecting the most suitable number of components to increase the performance in the classification of CASI imagery. The study concluded that minimum noise fraction (MNF) was the most suitable dimensionality reduction technique, which has also been supported by other authors (Melgani and Bruzzone 2004, Tarabalka et al. 2010, Ibarrola-Ulzurrun et al. 2017*c*).

Vegetation index masking

Once the pre-processing steps were completed, images with different spectral bands at 50 cm of spatial resolution providing reflectance values of the Earth surface were obtained. The next step was to create a mask to eliminate non-vegetation pixels. The reflectance curves (spectral signatures) for the different wavelengths of healthy green plants have a characteristic shape that is dictated by various plant attributes (Fig. 4).

Due to the characteristic vegetation spectral signature, vegetation indices are common to enhance vegetation information (Yamano et al. 2003). The normalized difference vegetation index (NDVI) (Rouse et al. 1974) and the modified soil-adjusted vegetation index (MSAVI2) (Huete 1988) are the most suitable for estimating quantitative characteristics of vegetation in dry and semi-dry regions (Galvão et al. 1999, Wang and Tenhunen 2004, Medina-Machín et al. 2019). NDVI is the ratio between the Red (RED) and the near-infrared (NIR) regions (Eq. 1), while MSAVI2 is a more complex index applied to areas with a high degree of exposed soil surface (Eq. 2).

$$\mathrm{NDVI} = \frac{(\mathrm{NIR} - \mathrm{RED})}{(\mathrm{NIR} + \mathrm{RED})} \tag{1}$$

$$\mathrm{MSAV}I2 = \frac{2\mathrm{NIR} + 1 - \sqrt{(2\mathrm{NIR} + 1)^2 - 8(\mathrm{NIR} - \mathrm{RED})}}{2} \tag{2}$$

After calculating both vegetation indices, boxplot analyses were obtained in order to select the most suitable vegetation index to distinguish between vegetation and non-vegetation areas. Then, the vegetation index threshold was used to create a mask to remove the non-vegetation pixels to subsequently classify vegetation areas at species level.

Classification

Remote sensing classification assigns a unique label to each pixel vector so that it is well-defined by a given class with a degree of uncertainty (Xie et al. 2008, Bioucas-Dias et al. 2013). The major steps involved in the classification step may include determination of a suitable classification system, such as selection of training samples, selection of a suitable classification model, and

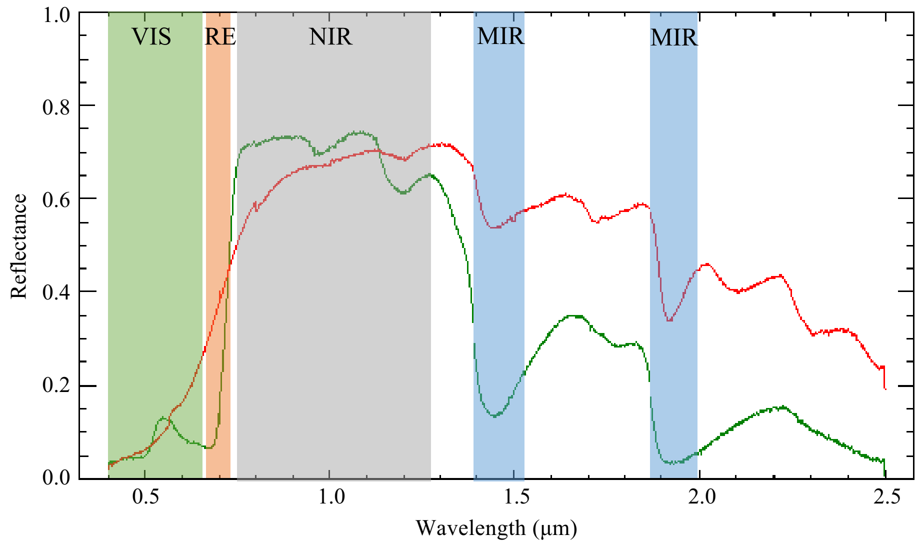

Fig. 4. Vegetation spectral signature. Green signature: healthy vegetation; red signature: dry vegetation. Shadowed areas: VIS, visible wavelength corresponding to the chlorophyll peak; RE, red edge; NIR, near-infrared wavelength corresponding with cell structure; MIR, middle infrared corresponding to the water absorption wavelengths.

accuracy assessment. The user needs the scale of the study area, the economic state, and the analyst skills, important factors influencing the selection of the data, the design of the classification procedure, and the quality of the classification results (Lu and Weng 2007).

Supervised classification methods are based on learning an established classification from a training dataset, which contains the predictor variables measured in each sampling unit and assigns prior classes to the sampling units (Xie et al. 2008). Training samples are usually collected from fieldwork or using images with fine spatial resolution. In the case of this study, several field observation campaigns were carried out to provide accurately located and quantitative ground reference data for each vegetation species of interest. Random sampling was used to select both training and testing regions of interest (ROIs) for the classification. This procedure was difficult to implement because of the variability of species spatial distribution and the small vegetation patches.

The first step in the classification process was to determine the classes appearing in the study area and obtain the database set of training and testing ROIs for each one. The classes were chosen according to criteria of representativity and abundance. The selected species were as follows: *S. supranubius*, *P. lasiospermus*, *D. bourgaeana,* and *P. canariensis* (Fig. 1). In order to obtain reliable classification maps, the training and testing samples were selected during the field observations in well-known sites around the study area.

Regarding the classification model, support vector machines (SVM) (Cortes and Vapnik 1995) have demonstrated their effectiveness in several remote sensing applications and in HS classification (Camps-Valls et al. 2008, Ballanti et al. 2016). SVM contain a machine learning algorithm that separates classes by defining the optimal hyperplane between them, based on support vectors that are defined by training data (Mountrakis et al. 2011). Specifically, several researches address the problem of very high-resolution classification by using SVM with a lower computational cost (Bruzzone and Carlin 2006, Ibarrola-Ulzurrun et al. 2017*b*, Xia et al. 2017). SVM was also selected because another previous study carried out in the same study area (Ibarrola-Ulzurrun et al. 2017*b*), comparing different algorithms, demonstrates the SVM capability to obtain accurate classification maps.

Evaluation of classification results is an important process in the mapping procedure. Thus, the

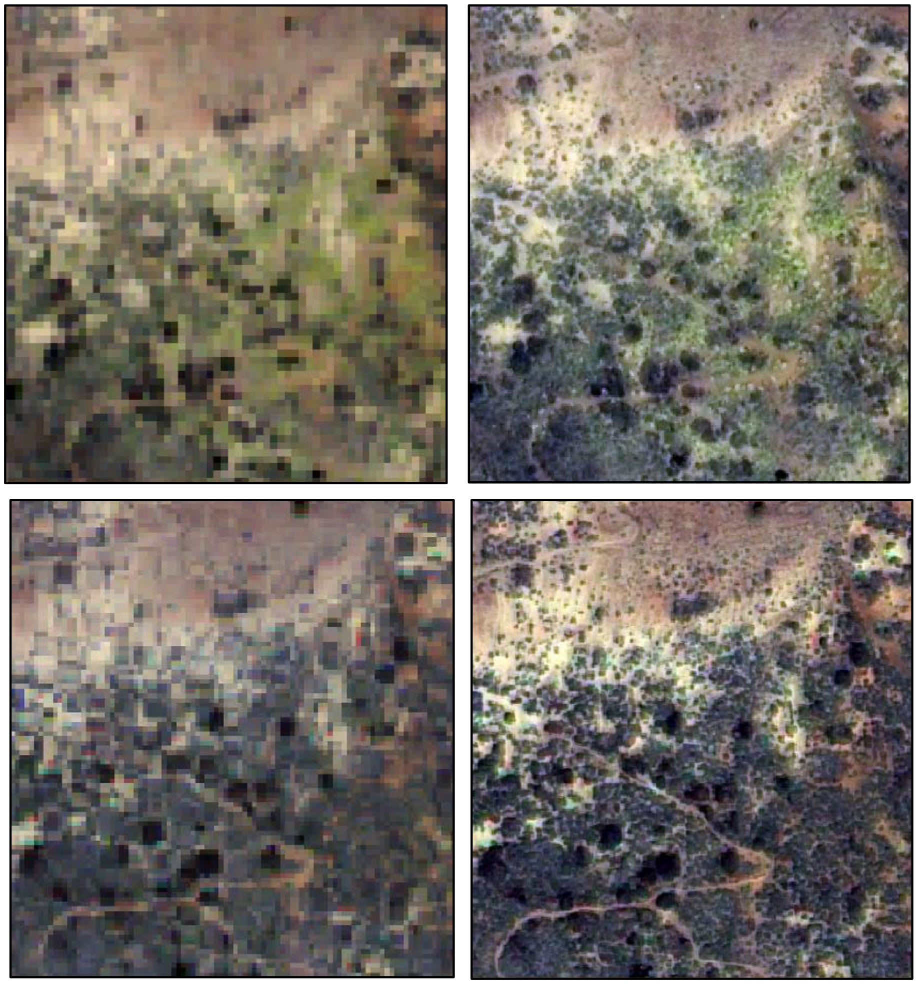

(a) (b)

Fig. 5. (a) Original multispectral image and (b) fused image. Top row: QuickBird images. Bottom row: WorldView-2 images.

statistical accuracy assessment used in the study was the standardized confusion error matrix. The confusion matrix approach is the most widely used and reports two global accuracy measurements, overall accuracy, and kappa coefficient. The kappa coefficient describes the proportion of correctly classified validation sites after random agreements are removed (Rosenfield and Fitzpatrick-Lins 1986). Moreover, it is recognized as a powerful method for analyzing a single error matrix and for comparing the differences between various error matrices (Lu and Weng 2007). Finally, combining classification with preliminary feature extraction and reduction techniques increases the classification accuracy.

Change detection analysis

The final step in the framework (Fig. 3) is the analysis of changes. After a revision of the state of the art of different change detection methods, the post-classification technique was decided as the most suitable method for the study. It is a useful technique for extracting land used and land-cover information, which independently classifies each image and compares the classified maps on a pixel-by-pixel basis to identify changes. Besides, it minimizes the impacts of atmospheric, sensor, and environmental differences between multi-temporal and multi-source images. Thus, no precise atmospheric correction is strictly required during the pre-processing of each scene. Moreover, it is useful because it provides details about changes and avoids selecting appropriate thresholds (Coppin et al. 2004, Alqurashi and Kumar 2013).

Results

Pre-processing results

After the radiometric and atmospheric corrections, the wavelet "*à trous*" pansharpening technique was applied. The spatial resolution obtained after the pansharpening step and the resizing was 0.5 m for both MS and HS imagery. Fig. 5 shows the spatial improvement of the MS bands and the importance of this step due to the small size of vegetation. Afterward, orthorectification was carried out, achieving an improved error around 2–2.5 m (reference image error ~36 m) (Fig. 6). Once both satellites images were orthorectified, a precise image co-registration was performed to almost achieve subpixel accuracy.

Regarding the dimensionality reduction of CASI imagery, a selection of the suitable components was carried out analyzing the eigenvalues and the standard deviation values of the entropy (Ibarrola-Ulzurrun et al. 2017*c*). Besides, a visual

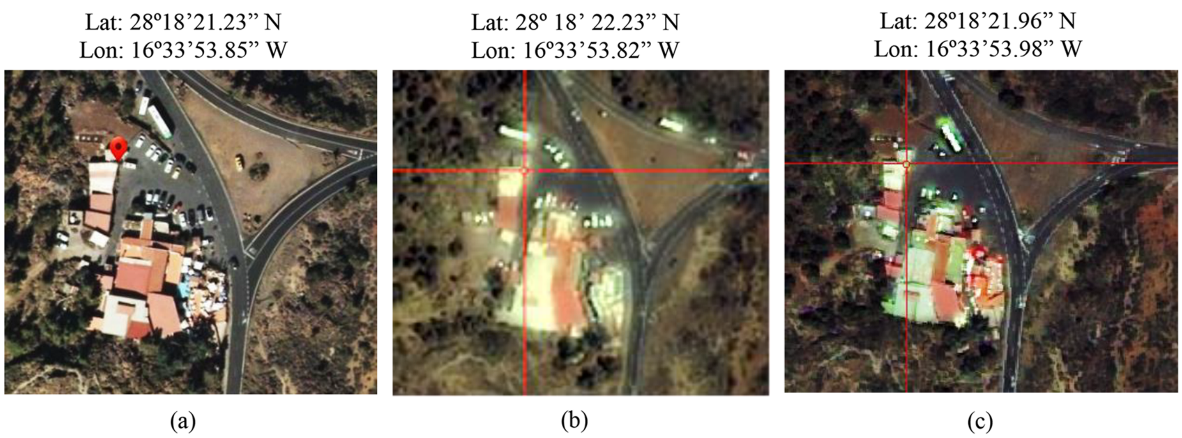

Fig. 6. (a) Orthophotograph of GRAFCAN and images after orthorectification: (b) QuickBird image and (c) WorldView-2 image.

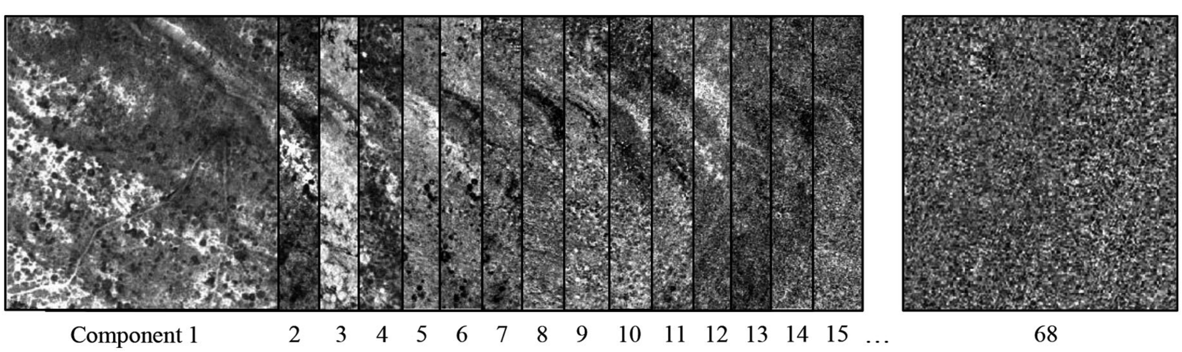

Fig. 7. Minimum noise fraction (MNF) components of the compact airborne spectrographic imager (CASI) image.

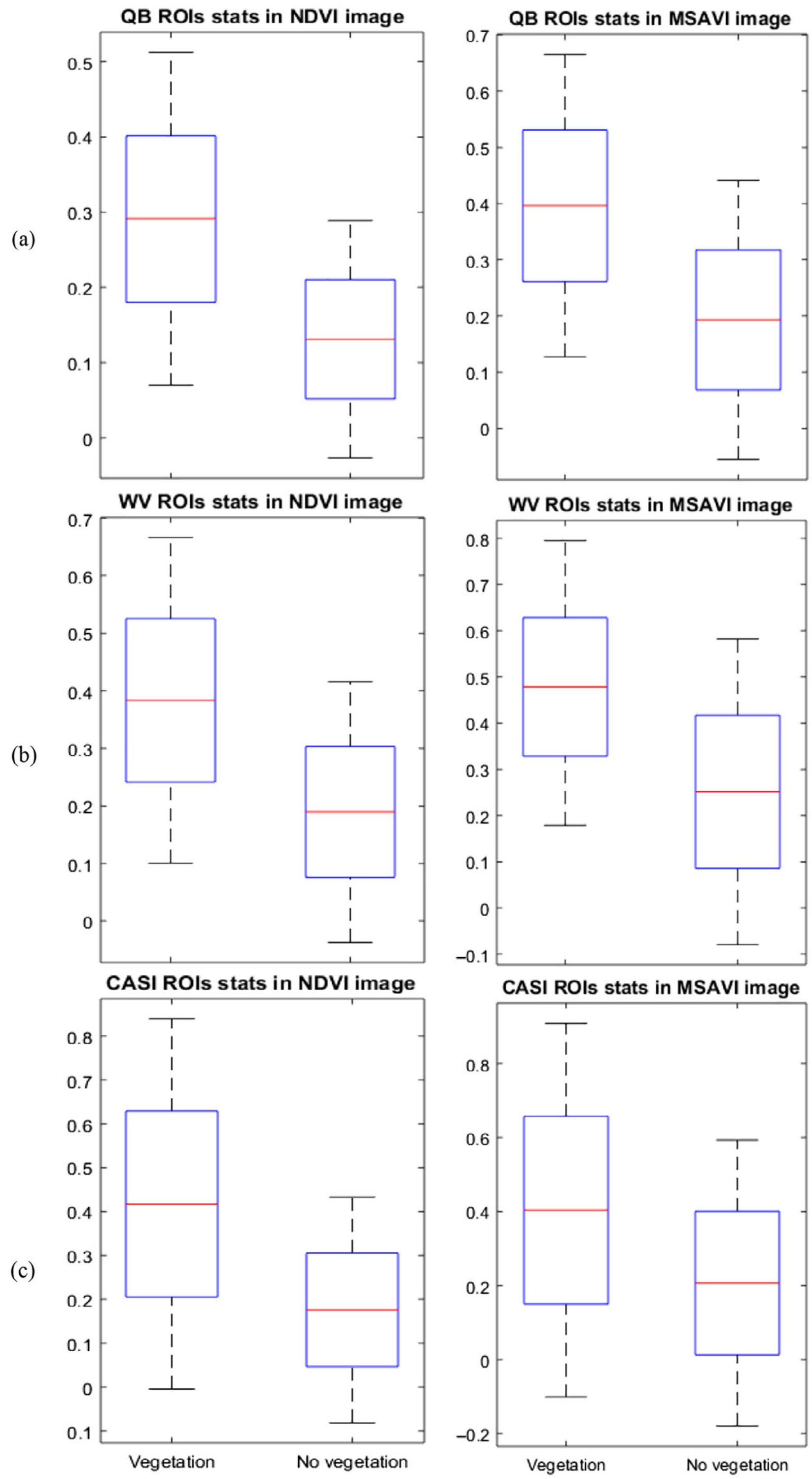

Fig. 8. Normalized difference vegetation index (NDVI) and modified soil-adjusted vegetation index (MSAVI2) boxplot diagrams for: (a) QuickBird (QB), (b) WorldView-2 (WV-2), and (c) compact airborne spectrographic imager (CASI).

assessment of the MNF components was made to determine which components are spatially coherent and which contain noise. Based on this procedure, a total of 8 components (Fig. 7) were chosen without losing relevant information for the vegetation classification for the final classification, instead of the original 68 bands.

Concerning the generation of a vegetation mask, analysis of NDVI and MSAVI-2 values was accomplished. Boxplot diagrams (Fig. 8) were obtained to study the behavior of NDVI and MSAVI2 values in vegetated (162,538 pixels) and non-vegetated (69,164 pixels) areas, covering the different plant species, as well as the different types of bare soil, road, and urban areas. The threshold was set in the first quartile of each index. Even though it was not possible to set an exact threshold to separate vegetated and non-vegetated areas, due to the spatial resolution of the imagery and to the presence of mixed pixels, NDVI more precisely discriminates vegetated and non-vegetated areas than MSAVI2. Therefore, NDVI was chosen to generate the vegetation mask configuration (Table 2).

Finally, Fig. 9 (top) shows the pre-processed and masked images used for the classification step. It can be appreciated how the vegetated area has increased from 2002 to 2017.

Table 2. Normalized difference vegetation index (NDVI) threshold to discriminate vegetated and non-vegetated areas in each image.

Image	Threshold
QB 2002	0.18
WV 2011	0.22
CASI 2017	0.20

Classification results

It is important to highlight the difficulty in classifying some types of vegetation due to the complexity of this heterogeneous shrubland ecosystem with mixed and small vegetation species such as *D. bourgaeana*. Hence, the major impact on the mapping of different types of vegetation is the misclassification created within the plant species, due to their spectral similarity and the mixing contributions from different covers in some pixels. Thus, it is important to create a reliable training sample database, which allows an accurate supervised classification to be made. This assumption leads us back to the importance of obtaining a fused image with the maximum spatial quality that allows to differentiate some small size species from others, avoiding pixel misclassification but also preserving the original spectral information.

A visual inspection of each classification was carried out to identify areas of potential error contrast between classifications. Moreover, the results of the classification were quantitatively assessed using the confusion matrices and the overall accuracy and kappa coefficient.

Table 3 shows the SVM classification overall accuracy and the kappa coefficient. It can be observed that accuracy increases depending on the type of imagery, being CASI imagery the most suitable sensor to obtain accurate thematic map, followed by WV-2 imagery. The main reason is the higher available number of spectral bands for the classification. Fig. 9 (down) presents the thematic maps for each scene. The increase in *S. supranubius* in 2015, followed by a decrease in 2017, was visually observed. *Pterocephalus lasiospermus* increases its coverage area from 2002 to 2017. *D. bourgaeana* seems to suffer a reduction of its cover area too, while *Pinus canariensis* remains stable.

Change detection analysis

Table 4 and Fig. 10 show the total vegetation and species coverage in the different years. Knowing the spatial resolution (0.5 m of pixel size) of each scene, it is possible to obtain specific coverage values in square kilometers. It is observed how the total vegetation has almost doubled since 2002. Moreover, it is demonstrated that *P. canariensis* and *D. bourgaeana* have barely changed their coverage area, as it was expected taking into account the previous works of Olano et al. (2017) and Cubas et al. (2018). On the other hand, *Pterocephalus lasiospermus* has increased from 2002 to 2017, tripling its initial extent in the last 15 yr; while *S. supranubius* has experienced an increase of 0.032 km^2 from 2002 to 2011, however, its population has decreased by 2017 to lower values than in 2002, with a net loss of 0.014 km^2 in the 15 yr analyzed.

The results are influenced by the many factors such as sensor spatial resolution, mixing of species, and classification accuracies. However, they

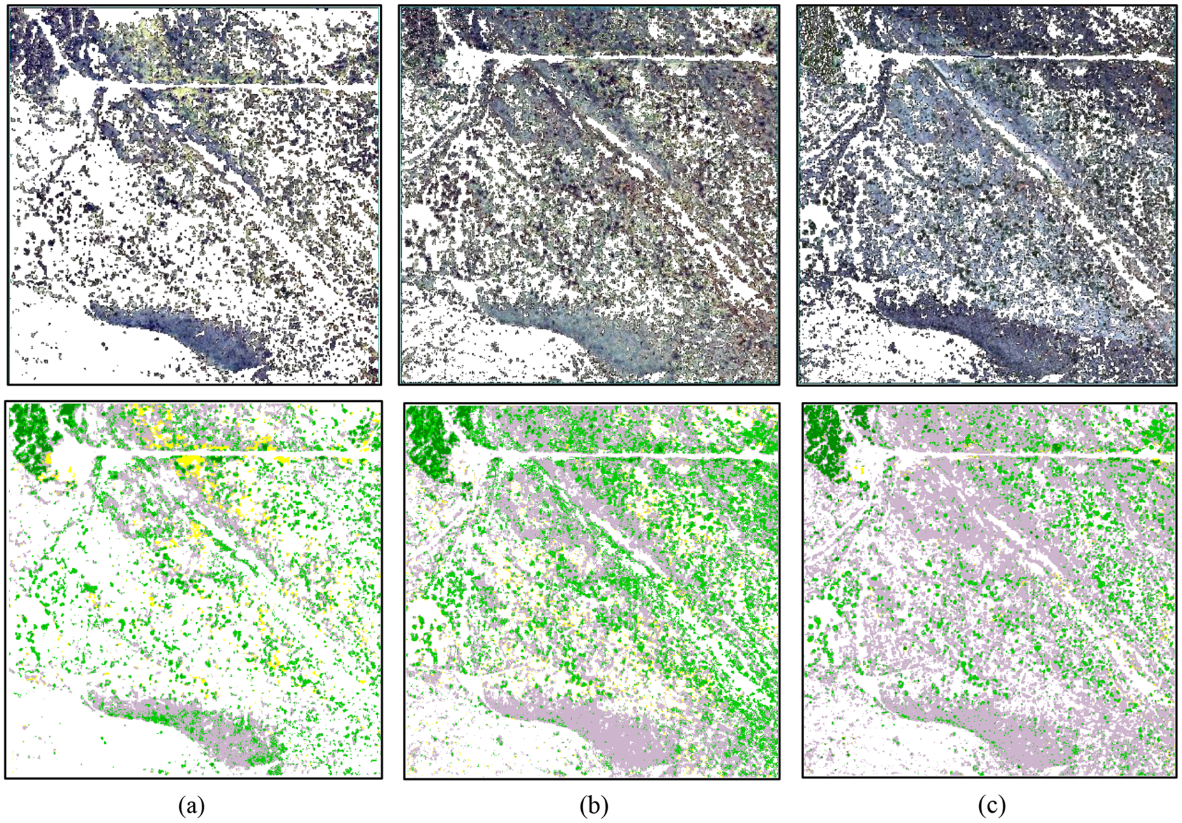

Fig. 9. Top row: Masked and pre-processed images: (a) QuickBird (QB), (b) WorldView-2 (WV-2), and (c) compact airborne spectrographic imager (CASI). Bottom row: Classification maps: (a) QuickBird, (b) WorldView-2, and (c) compact airborne spectrographic imager (CASI) imagery (light green, *Spartocytisus supranubius*; dark green, *Pinus canariensis*; violet, *Pterocephalus lasiospermus*; yellow, *Descurainia bourgaeana*).

Table 3. Support vector machine (SVM) classification overall accuracy and kappa coefficient.

Image	Overall accuracy (%)	Kappa coefficient
QB	77.99	0.632
WV-2	85.03	0.741
CASI	95.77	0.922

provide quite accurate information about the dynamics of the Teide ecosystem and it is possible to obtain reasonable trends of the vegetation changes in the habitat.

Table 4. Vegetation and plant species coverage in the different scenes.

	QB 2002		WV 2011		CASI 2017	
Species	%	km^2	%	km^2	%	km^2
Total vegetation	31.33	0.215	56.61	0.388	59.38	0.407
Pinus canariensis	1.16	0.008	1.24	0.009	1.90	0.013
Spartocytisus supranubius	11.69	0.080	16.35	0.112	9.65	0.066
Pterocephalus lasiospermus	15.83	0.109	34.05	0.234	47.16	0.323
Descurainia bourgaeana	2.66	0.018	4.97	0.034	0.68	0.005

Discussion

A complex ecosystem, with mixed vegetation and small size, was analyzed using remote sensing data, being a challenging methodological framework. Specifically, it was observed the necessity to perform accurate pre-processing steps in order to improve the spectral and spatial quality of the imagery. Vegetation indices were

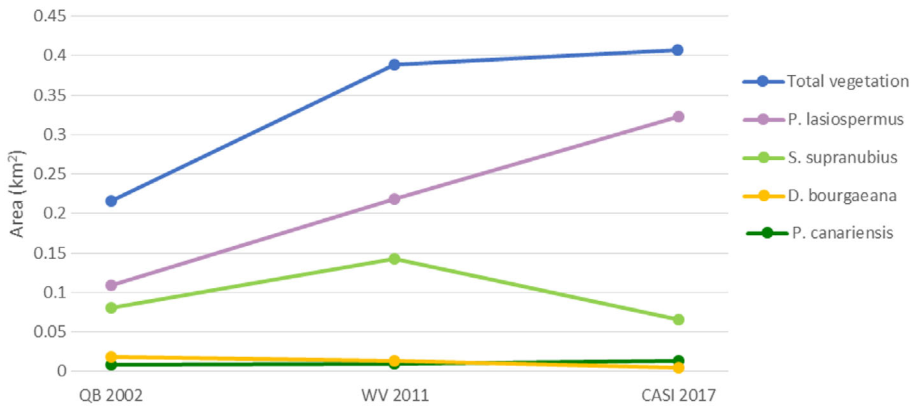

Fig. 10. Vegetated area and plant species coverage in 2002, 2011, and 2017 in the different scenes.

also applied to improve the final mapping accuracy. After performing the specific pre-processing steps, it was possible to obtain quite reliable thematic maps applying the SVM algorithm, properly trained and parameterized, which were used for the change detection study.

Multi-source and multi-temporal remote sensing imagery were used to complement and add accurate information to field observations for a future ecosystem management. Important outcomes of the study are the increase in the coverage of vegetation (practically doubled) in 15 yr, the dominance of *Pterocephalus lasiospermus* whose extension has almost tripled, and the decline of *S. supranubius* (despite the rebound of 2011), corroborating the works by Olano et al. (2017) and Cubas et al. (2018), for specific test locations. It surprises the rapid expansion of *P. lasiospermus*, a very rare species several decades ago, whose current predominance is accelerated vigorously, altering the landscape in this sector of the high mountain ecosystem. Undoubtedly, the aforementioned facilitating effect of herbivores, their better resistance to herbivory, and their own thermophilic character are factors that help explaining their considerable increase in a warming scenario.

Thanks to remote sensing, it has been possible to study those changes in a larger area, as well as obtaining quantitative results of how the species coverage and location have changed during years. However, some advanced tasks have to be undertaken before satisfactory results can be achieved (i.e., suitable data, pre-processing, develop accurate classification models, knowledge of the study area, and time and cost restrictions). In conclusion, the remote sensing framework proposed is ecologically relevant, statistically credible, cost-effective, flexible, and transferable to other systems giving a guidance to environmental managers to consider remote sensing as a useful tool. Moreover, hints and advices are given to facilitate the framework application to other habitats and ecosystems.

Future studies will include the systematic change detection monitoring in the whole Teide National Park, using WorldView-2 and WorldView-3 imagery, in order to obtain more accurate results and with a continuity during years. Moreover, vegetation features, habitat heterogeneity, species richness, and species–area relationships can be extracted from this study. Thus, specific research plans could be implemented following the proposed framework.

Acknowledgments

This research has been supported by the ARTEMISAT-2 (CTM2016-77733-R) project, which was funded by the Spanish Agencia Estatal de Invetigación (AEI) and by the Fondo Europeo de Desarrollo Regional (FEDER). This work was completed while E. I-U was a PhD student in the IOCAG Doctoral Program in Oceanography and Global Change (ULPGC), and it was funded by the Spanish Ministerio de Economía y Competitividad with a FPI grant (BES-2014-069426).

Literature Cited

Alqurashi, A. F., and L. Kumar. 2013. Investigating the use of remote sensing and GIS techniques to detect land use and land cover change: a review. Advances in Remote Sensing 2:193.

Aplin, P. 2004. Remote sensing: land cover. Progress in Physical Geography 28:283–293.

Ballanti, L., L. Blesius, E. Hines, and B. Kruse. 2016. Tree species classification using hyperspectral imagery: a comparison of two classifiers. Remote Sensing 8:445.

Bioucas-Dias, J. M., A. Plaza, G. Camps-Valls, P. Scheunders, N. Nasrabadi, and J. Chanussot. 2013. Hyperspectral remote sensing data analysis and future challenges. IEEE Geoscience and Remote Sensing Magazine 1:6–36.

Brito, P., J. R. Lorenzo, Á. M. González-Rodríguez, D. Morales, G. Wieser, and M. S. Jimenez. 2014. Canopy transpiration of a *Pinus canariensis* forest at the tree line: implications for its distribution under predicted climate warming. European Journal of Forest Research 133:491–500.

Bruzzone, L., and L. Carlin. 2006. A multilevel context-based system for classification of very high spatial resolution images. IEEE Transactions on Geoscience and Remote Sensing 44:2587–2600.

Camps-Valls, G., L. Gómez-Chova, J. Muñoz-Marí, J. L. Rojo-Álvarez, and M. Martínez-Ramón. 2008. Kernel-based framework for multitemporal and multisource remote sensing data classification and change detection. IEEE Transactions on Geoscience and Remote Sensing 46:1822–1835.

Chapuis, J.-L., Y. Frenot, and M. Lebouvier. 2004. Recovery of native plant communities after eradication of rabbits from the subantarctic Kerguelen Islands, and influence of climate change. Biological Conservation 117:167–179.

Coppin, P., I. Jonckheere, K. Nackaerts, and B. Muys. 2004. Digital change detection methods in ecosystem monitoring: a review. International Journal of Remote Sensing 25:1565–1596.

Corbane, C., S. Alleaume, and M. Deshayes. 2013. Mapping natural habitats using remote sensing and sparse partial least square discriminant analysis. International Journal of Remote Sensing 34:7625–7647.

Cortes, C., and V. Vapnik. 1995. Support vector machine. Machine Learning 20:273–297.

Cubas, J., J. L. Martín-Esquivel, M. Nogales, S. D. Irl, R. Hernández-Hernández, M. López-Darias, M. Marrero-Gómez, M. J. del Arco, and J. M. González-Mancebo. 2018. Contrasting effects of invasive rabbits on endemic plants driving vegetation change in a subtropical alpine insular environment. Biological Invasions 20:793–807.

de Miguel, E., A. Fernández-Renau, E. Prado, M. Jiménez, Ó. G. de la Cámara, C. Linés, J. A. Gómez, A. I. Martín, and F. Muñoz. 2014. The processing of CASI-1500I data at INTA PAF. EARSeL eProceedings 13:30–37.

del Arco Aguilar, M.-J., R. González-González, V. Garzón-Machado, and B. Pizarro-Hernández. 2010. Actual and potential natural vegetation on the Canary Islands and its conservation status. Biodiversity and Conservation 19:3089–3140.

ENVI. 2004. ENVI user's guide. Harris Geospatial Solutions, Broomfield, Colorado, USA.

Fauvel, M., Y. Tarabalka, J. A. Benediktsson, J. Chanussot, and J. C. Tilton. 2013. Advances in spectral-spatial classification of hyperspectral images. Proceedings of the IEEE 101:652–675.

Feilhauer, H., F. Thonfeld, U. Faude, K. S. He, D. Rocchini, and S. Schmidtlein. 2013. Assessing floristic composition with multispectral sensors—A comparison based on monotemporal and multi-seasonal field spectra. International Journal of Applied Earth Observation and Geoinformation 21:218–229.

Förster, M., M. Zebisch, I. Wagner-Lücker, T. Schmidt, K. Renner, and M. Neubert. 2014. Remote sensing-based monitoring of potential climate-induced impacts on habitats. Pages 95–113 *in* S. Rannow and M. Neubert, editors. Managing protected areas in Central and Eastern Europe under climate change. Springer, Dordrecht, The Netherlands.

Galvão, L. S., Í. Vitorello, and R. Almeida Filho. 1999. Effects of band positioning and bandwidth on NDVI measurements of tropical savannas. Remote Sensing of Environment 67:181–193.

Ghamisi, P., J. A. Benediktsson, and S. Phinn. 2015. Land-cover classification using both hyperspectral and LiDAR data. International Journal of Image and Data Fusion 6:189–215.

Ghamisi, P., J. Plaza, Y. Chen, J. Li, and A. J. Plaza. 2017. Advanced spectral classifiers for hyperspectral images: a review. IEEE Geoscience and Remote Sensing Magazine 5:8–32.

Gong, M., P. Zhang, L. Su, and J. Liu. 2016. Coupled dictionary learning for change detection from multisource data. IEEE Transactions on Geoscience and Remote Sensing 54:7077–7091.

González-Rodríguez, Á. M., P. Brito, J. R. Lorenzo, A. Gruber, W. Oberhuber, and G. Wieser. 2017. Seasonal cycles of sap flow and stem radius variation of *Spartocytisus supranubius* in the alpine zone of Tenerife, Canary Islands. Alpine Botany 127:97–108.

Huete, A. R. 1988. A soil-adjusted vegetation index (SAVI). Remote Sensing of Environment 25:295–309.
Hughes, G. 1968. On the mean accuracy of statistical pattern recognizers. IEEE Transactions on Information Theory 14:55–63.
Ibarrola-Ulzurrun, E., C. Gonzalo-Martin, J. Marcello-Ruiz, A. Garcia-Pedrero, and D. Rodriguez-Esparragon. 2017*a*. Fusion of high resolution multispectral imagery in vulnerable coastal and land ecosystems. Sensors 17:228.
Ibarrola-Ulzurrun, E., C. Gonzalo-Martín, and J. Marcello. 2017*b*. Influence of pansharpening in obtaining accurate vegetation maps. Canadian Journal of Remote Sensing 43:528–544.
Ibarrola-Ulzurrun, E., J. Marcello, and C. Gonzalo-Martin. 2017*c*. Assessment of component selection strategies in hyperspectral imagery. Entropy 19:666.
Ibarrola-Ulzurrun, E., J. Marcello, and C. Gonzalo-Martin. 2018. Advanced classification of remote sensing high resolution imagery: an application for the management of natural resources. Pages 1–13 *in* Á. Rocha and L. Reis, editors. Developments and advances in intelligent systems and applications. Springer, Cham, Switzerland.
Jianya, G., S. Haigang, M. Guorui, and Z. Qiming. 2008. A review of multi-temporal remote sensing data change detection algorithms. International Archives of the Photogrammetry, Remote Sensing and Spatial Information Sciences 37:757–762.
Jiménez-Michavila, M. 2011. Cartografía de especies de matorral de la Reserva Biológica de Doñana mediante el sistema hiperespectral aeroportado INTA-AHS. Implicaciones en el estudio y seguimiento del matorral de Doñana. Universidad Autónoma de Madrid, Madrid, Spain.
Lausi, D., and P. L. Nimis. 1986. Leaf and canopy adaptations in a high-elevation desert on Tenerife, Canary Islands. Vegetatio 68:19–31.
Lu, D., P. Mausel, E. Brondizio, and E. Moran. 2004. Change detection techniques. International Journal of Remote Sensing 25:2365–2401.
Lu, D., and Q. Weng. 2007. A survey of image classification methods and techniques for improving classification performance. International Journal of Remote Sensing 28:823–870.
Manley, P. N., W. J. Zielinski, C. M. Stuart, J. J. Keane, A. J. Lind, C. Brown, B. L. Plymale, and C. O. Napper. 2000. Monitoring ecosystems in the Sierra Nevada: the conceptual model foundation. Environmental Monitoring and Assessment 64:139–152.
Marcello, J., F. Eugenio, U. Perdomo, and A. Medina. 2016. Assessment of atmospheric algorithms to retrieve vegetation in natural protected areas using multispectral high resolution imagery. Sensors 16: 1624.
Martín, J. L., J. Bethencourt, and E. Cuevas-Agulló. 2012. Assessment of global warming on the island of Tenerife, Canary Islands (Spain): trends in minimum, maximum and mean temperatures since 1944. Climatic Change 114:343–355.
Mason, T., D. Keith, and A. Letten. 2017. Detecting state changes for ecosystem conservation with long-term monitoring of species composition. Ecological Applications 27:458–468.
Medina-Machín, A., J. Marcello, A. Hernández-Cordero, J. Martín-Abasolo, and F. Eugenio. 2019. Vegetation species mapping in a coastal-dune ecosystem using high resolution satellite imagery. GIScience & Remote Sensing 56:210–232.
Melgani, F., and L. Bruzzone. 2004. Classification of hyperspectral remote sensing images with support vector machines. IEEE Transactions on Geoscience and Remote Sensing 42:1778–1790.
Mouat, D. A., G. G. Mahin, and J. Lancaster. 1993. Remote sensing techniques in the analysis of change detection. Geocarto International 8:39–50.
Mountrakis, G., J. Im, and C. Ogole. 2011. Support vector machines in remote sensing: a review. ISPRS Journal of Photogrammetry and Remote Sensing 66:247–259.
Mueller, M., and J. Geist. 2016. Conceptual guidelines for the implementation of the ecosystem approach in biodiversity monitoring. Ecosphere 7:e01305.
Nunez-Casillas, L., F. Micand, B. Somers, P. Brito, and M. Arbelo. 2012. Plant species monitoring in the Canary Islands using WorldView-2 imagery. ISPRS-International Archives of the Photogrammetry. Remote Sensing and Spatial Information Sciences XXXIX-B8:301–304.
Olano, J. M., P. Brito, Á. M. González-Rodríguez, J. L. Martín-Esquivel, M. García-Hidalgo, and V. Rozas. 2017. Thirsty peaks: Drought events drive keystone shrub decline in an oceanic island mountain. Biological Conservation 215:99–106.
Pepin, N., and J. Lundquist. 2008. Temperature trends at high elevations: patterns across the globe. Geophysical Research Letters 35:L14701.
Perera-Castro, A., P. Brito, and A. González-Rodríguez. 2017*a*. Changes in thermic limits and acclimation assessment for an alpine plant by chlorophyll fluorescence analysis: Fv/Fm vs. Rfd. Photosynthetica. http://riull.ull.es/xmlui/handle/915/4460
Perera-Castro, A. V., P. Brito, and A. M. Gonzalez-Rodriguez. 2017*b*. Light response in alpine species: different patterns of physiological plasticity. Flora 234:165–172.

Petit, C., and E. Lambin. 2001. Integration of multi-source remote sensing data for land cover change detection. International Journal of Geographical Information Science 15:785–803.

Rodriguez-Galiano, V., M. Chica-Olmo, F. Abarca-Hernandez, P. Atkinson, and C. Jeganathan. 2012. Random forest classification of Mediterranean land cover using multi-seasonal imagery and multi-seasonal texture. Remote Sensing of Environment 121:93–107.

Rosenfield, G. H., and K. Fitzpatrick-Lins. 1986. A coefficient of agreement as a measure of thematic classification accuracy. Photogrammetric Engineering and Remote Sensing 52:223–227.

Rouse Jr., J. W., R. Haas, J. Schell, and D. Deering. 1974. Monitoring vegetation systems in the Great Plains with ERTS. Pages 309–317 *in* S. C. Freden, E. P. Mercanti, and M. A. Becker, editors. Third earth resources technology satellite-1 symposium. Volume I: technical presentations. NASA SP-351. NASA, Washington, D.C., USA.

Singh, A. 1989. Review article digital change detection techniques using remotely-sensed data. International Journal of Remote Sensing 10:989–1003.

Spanhove, T., J. V. Borre, S. Delalieux, B. Haest, and D. Paelinckx. 2012. Can remote sensing estimate fine-scale quality indicators of natural habitats? Ecological Indicators 18:403–412.

Sventenius, E. R. 1946. Notas sobre la flora de Las Cañadas de Tenerife. Instituto Nacional de Investigaciones Agronómicas, Centro de las Islas Canarias.

Tarabalka, Y., J. Chanussot, and J. A. Benediktsson. 2010. Segmentation and classification of hyperspectral images using watershed transformation. Pattern Recognition 43:2367–2379.

Volpi, M., D. Tuia, F. Bovolo, M. Kanevski, and L. Bruzzone. 2013. Supervised change detection in VHR images using contextual information and support vector machines. International Journal of Applied Earth Observation and Geoinformation 20:77–85.

Wang, Q., and J. D. Tenhunen. 2004. Vegetation mapping with multitemporal NDVI in North Eastern China transect (NECT). International Journal of Applied Earth Observation and Geoinformation 6:17–31.

Xia, J., N. Falco, J. A. Benediktsson, P. Du, and J. Chanussot. 2017. Hyperspectral image classification with rotation random forest via KPCA. IEEE Journal of Selected Topics in Applied Earth Observations and Remote Sensing 10:1601–1609.

Xie, Y., Z. Sha, and M. Yu. 2008. Remote sensing imagery in vegetation mapping: a review. Journal of Plant Ecology 1:9–23.

Yamano, H., J. Chen, and M. Tamura. 2003. Hyperspectral identification of grassland vegetation in Xilinhot, Inner Mongolia, China. International Journal of Remote Sensing 24:3171–3178.